Eliminating Starting Hesitation for Reliable Sensorless Control of Switched Reluctance Motors

Jianrong Bu, *Member, IEEE*, and Longya Xu, *Senior Member, IEEE*

***Abstract*—Novel methods for rotor position estimation both at standstill and during running conditions are presented for a switched reluctance machine (SRM) starting free of position sensor and hesitation. By applying a dc pulse to the stator phase windings for a short moment (0.5 ms), the initial rotor position can be accurately detected. Combining the accurate initial rotor position with a novel rotor position estimation algorithm during running, the SRM can be started at any initial rotor position without starting hesitation. Critical issues related to optimal model selection as the virtual sensor are discussed in detail. Computer simulation and experimental results are included.**

***Index Terms*—Fuzzy logic, motor, sensorless control, switched reluctance.**

I. Introduction

HIGH-PERFORMANCE switched reluctance machine (SRM) drives require accurate rotor position both at standstill and during running conditions. The accurate rotor position is especially significant for wide speed range applications where both magnitude and phase angle of current have to be precisely controlled. Rotor position can be directly measured by a rotor position sensor. However, mounting the rotor position sensor increases the size and cost of the overall system. The rotor position sensor is also a source of unreliability in situations such as high speed, high temperature, or where electromagnetic interference presents. Another problem of using a rotor position sensor is the rotor starting hesitation associated with the uncertainty of initial rotor position. The rotor starting hesitation is strictly not allowed in high-performance servo systems. To remove the rotor position sensor, considerable attention has recently been paid to indirect rotor position estimation [1]–[11]. However, the rotor starting hesitation problem remains in almost all rotor position estimation algorithms thus far.

Critical issues related to high-performance rotor position sensorless control of SRMs without starting hesitation are investigated in this paper. Following the detailed description of starting hesitation, model selection for SRM rotor position estimation at standstill and during running conditions is first discussed. Then, novel methods for rotor position estimation both at standstill and during running conditions are presented. Based on the rotor position estimation methods, a reliable starting procedure without rotor starting hesitation is proposed. Computer simulation and experimental results are provided to substantiate the effectiveness of the proposed algorithms. Conclusions are made accordingly.

Paper IPCSD 00–044, presented at the 1998 Industry Applications Society Annual Meeting, St. Louis, MO, October 12–16, and approved for publication in the IEEE TRANSACTIONS ON INDUSTRY APPLICATIONS by the Industrial Drives Committee of the IEEE Industry Applications Society. Manuscript submitted for review October 15, 1998 and released for publication October 25, 2000.

J. Bu was with the Electrical Engineering Department, The Ohio State University, Columbus, OH 43210 USA. He is now with Emerson Motion Control, Eden Prairie, MN 55344-3620 USA (e-mail: Jianrong.Bu@emersondrivesolutions.com).

L. Xu is with the Electrical Engineering Department, The Ohio State University, Columbus, OH 43210 USA (e-mail: xu.12@osu.edu).

Publisher Item Identifier S 0093-9994(01)00904-5.

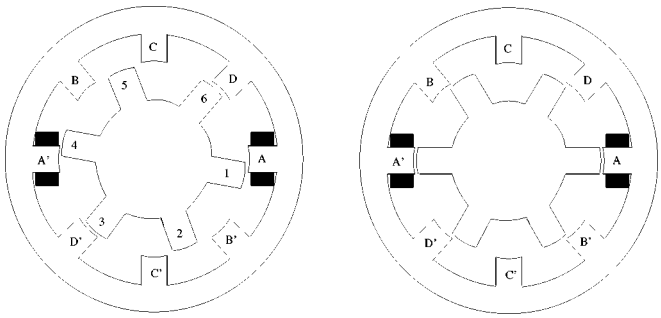

Fig. 1. An 8/6 SRM.

II. Analysis of SRM Starting Hesitation

The rotor starting hesitation can be understood by examining the following starting process with a rotor position sensor. To ensure that the SRM rotates in a desired direction, the initial rotor position must be known. In an SRM with a conventional rotor position sensor (resolves or optical encoders), rather than measuring the initial rotor position, rotor position initialization (or alignment) is done before starting. In this case, the dc-bus voltage is applied to a stator phase (for example, phase A) for a brief moment to pull the rotor to the aligned position with respect to a pair of stator poles as shown in Fig. 1. After the pair of stator and rotor poles are aligned, appropriate starting of the SRM can be launched in the desired rotation direction. For a clockwise rotation, phase D is excited, otherwise, phase B. It is clear that during the rotor initialization process, the rotor could move toward the undesired direction, resulting in starting hesitation. The starting hesitation can be found in other cases as well.

- To pull a rotor with a large inertia into alignment with the stator poles, the initialization current generally has to be

large. The large current causes the rotor to overshoot and vibrate around the aligned rotor position, which usually takes more than 0.5 s, resulting in substantial starting hesitation.

- Before the SRM rotor is pulled to the aligned position, the rotor may be in a neutral position. For example, in Fig. 1, the rotor is in a neutral position relative to phase C. If phase C is used for initialization, either rotor pole 5 or 6 could be attracted to the aligned rotor position. In the worst case, the rotor may be locked and never be pulled to the aligned rotor position if the SRM is completely symmetrical.

Many technical papers discussing the topic of sensorless control have been published, but few have discussed rotor starting hesitation. A rotor position initialization process similar to that in controlling an SRM with a sensor is applied in most sensorless control algorithms. The sensorless control methods could be based on either chopped current waveforms [1], [2] or diagnostic pulses [7], [8]. Obviously, the chopped current method cannot be used to find the initial rotor position at standstill and, hence, to eliminate starting hesitation. On the other hand, by applying diagnostic pulses to a phase winding, the rotor positions at standstill and in running may be estimated. However, the mutual coupling among the phases prevents this method from being effective once the SRM is running at high speeds [3]. An open-loop method can also be used to start an SRM [6]. Assuming that clockwise rotation is desired, the phase excitation sequence should be A–D–C–B–A according to Fig. 1 regardless of the initial rotor position. The open-loop method excites the phase windings in the above sequence with the appropriate frequency. After the rotor reaches a threshold rotor speed, the rotor position estimation method then is activated. However, like any open-loop method, the above method is sensitive to load conditions and is unreliable. It cannot guarantee the elimination of starting hesitation either.

III. Sensorless Control Without Starting Hesitation

A. Model Selection for Rotor Position Estimation

As the first step in developing SRM sensorless control algorithms without starting hesitation, the model selected for rotor position estimation is critically important. The general principles for most SRM rotor position estimation methods are based on the measurement of phase current "i" and flux linkage "λ" (or phase inductance "L"), and the preknown magnetizing characteristics [12]. That is, at a given instant, if the phase current and flux linkage (or inductance) are known, the rotor position can be uniquely determined from the preknown magnetizing characteristics. Two types of SRM models are usable for rotor position estimation. The first type describes an SRM in terms of the relationships among phase flux linkage, current, and rotor position, and the second type uses phase inductance, current, and rotor position. The first type is much preferred because the computation or measurement of flux linkage is more direct and simpler than that of inductance.

Fig. 2 shows the measured relationships among phase flux linkage, current, and rotor position for an eight-stator/six-rotor-pole (8/6) SRM. In this figure, except for the "$*$" and "$+$" curves, the rotor position difference between any two adjacent curves is 3°. Because the curves are directly measured under the actual operating conditions, all factors including rotor positions, current levels, saturation, and mutual coupling are considered naturally. The top and bottom curves in the figure correspond to the magnetizing characteristics at aligned and unaligned rotor positions. If the unaligned rotor position is defined as 0°, the "$*$" curve corresponds to the magnetizing characteristics at 5° and the "$+$" curve at 25°. According to the "$*$" and "$+$" marks, the whole range of magnetizing characteristics of the SRM is divided into three regions; region R1 above the "$+$" curve, region R2 between the "$+$" and "$*$" curves, and region R3 below the "$*$" curve. From Fig. 2, it can be observed that every pair of values of phase flux linkage and current specifies a unique rotor position. However, utilizing the family of λ–i curves to derive the rotor position, the estimation has very different accuracies in different regions. In regions R1 and R3, because the adjacent curves are very close to each other, the rotor position estimation accuracy is low, and small errors in flux linkage and/or current measurement can result in a large error in rotor position estimation. In contrast, the rotor position estimation accuracy is high in region R2, and small errors in flux linkage and/or current only result in a negligible estimation error, because for the same amount of incremental rotor position difference (3°), the curves are separated widely in the λ–i plane. From the λ–i curves, it is also clear that sufficient current value is needed for accurate rotor position estimation. Therefore, a good estimation method should conduct the rotor position estimation in region R2 with an adequate phase current.

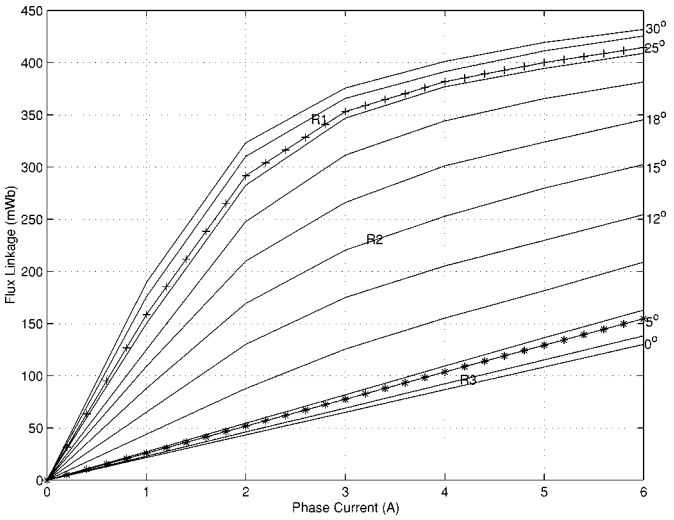

Fig. 2. Magnetizing characteristics of an 8/6 SRM.

B. Rotor Position Detection at Standstill

From the discussion in Section II, it is clear that, to eliminate starting hesitation, it is necessary to obtain information about the rotor position without initializing and disturbing the rotor at standstill. The method of eliminating starting hesitation presented in this paper is based on the initial rotor position estimation realized in the following steps.

1) Excite all phases for a very short moment (0.5 ms).
2) Find the phase having the largest current.

3) Choose a phase next to the phase having the largest current to be the optimal phase for the rotor position estimation. In theory, the phase either right or left next to the phase with the largest current can be chosen as the optimal phase. To avoid ambiguity, the right phase is always chosen as the optimal phase in this paper. For example, if phase A has the largest current, phase B is chosen to be the optimal phase.
4) Compute the flux linkage for the chosen optimal phase.
5) Estimate the initial rotor position from a prestored magnetizing characteristics table based on the current and flux linkage of the chosen optimal phase.

The success of this method lies in step 3). The phase with the largest phase current has the smallest phase inductance, which indicates that the initial rotor position relative to this phase is very close to the totally unaligned position. On the other hand, the phase with the smallest phase current has the largest phase inductance, which indicates that the initial rotor position to this phase is very close to the totally aligned position. As explained in Section III-A, in the regions (R1 and R3) close to the aligned and unaligned rotor positions, the rotor position estimation accuracy is low. Thus, the phase with either the largest current to the smallest current is not suitable for accurate rotor position estimation. Looking at Fig. 1(a) and (b), it can be observed that the phase next to the phase with largest current has medium inductance, and the possible rotor position relative to this medium inductance will be between 7.5°–22.5°. Thus, the phase next to the phase with the largest current is the best candidate phase for initial rotor position estimation because the rotor position will be conducted in the high position estimation resolution region R2 as indicated in Fig. 2.

The above estimation method has the following salient features.

1) Estimation is done in the high-resolution region: Assuming that phase C has the largest current, then phase D will be selected as the optimal phase for initial rotor position estimation. As explained above, the possible initial rotor position relative to the axis of phase D will be between 7.5°–22.5° where high position estimation resolution is expected.
2) Diagnostic signal is sufficient. If phase C has the largest current, the current in phase D will be large and sufficient for accurate initial rotor position estimation.
3) Flux linkage computation is simple and accurate. At standstill, the back electromotive force (EMF) in any phase winding is zero. Therefore, the phase current during the excitation can be determined by the following equation:

$$i(t) = \frac{V}{R}(1 - e^{-(R/L)t}) \tag{1}$$

where V is the dc-bus voltage, R is the phase resistance, and L is the phase inductance at initial rotor position. If the excitation duration Δt is short (much less than the inverse of time constant R/L), the phase current will increase linearly. Therefore, the flux linkage in phase D can be calculated by

$$\lambda_D(\Delta t) = \left\{V - \tfrac{1}{2}\, R i_D(\Delta t)\right\} \Delta t \tag{2}$$

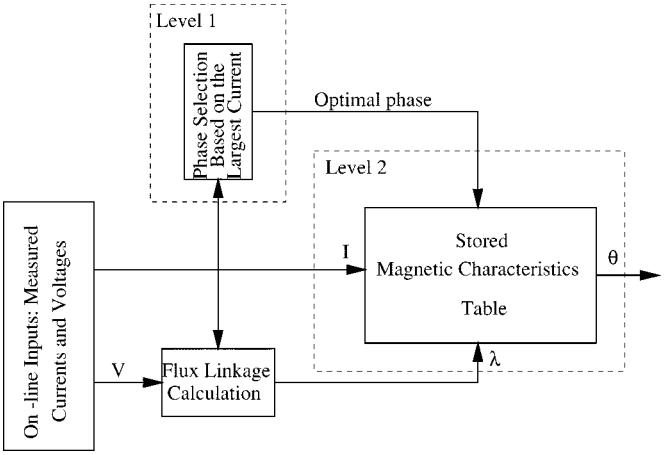

Fig. 3. Position estimation during running.

where i_D is the measured current in phase D while λ_D is estimated at the end of Δt. Notice that complicated integration for flux linkage computation is not needed here and a single-step computation achieves the flux linkage of interest.

It should be pointed out that to obtain accurate initial rotor position, the duration of excitation should be adequate to build up an appropriate amount of phase current. However, the duration of excitation should not be too long, or the initial rotor position of the SRM will be disturbed. In this paper, the current from the excitation is about half of the rated current, and the initial rotor position estimation completes in 0.54 ms. No extra hardware is needed to find the initial rotor position.

C. Rotor Position Estimation During Running

With the known initial rotor position, it is straightforward to determine the sequence of phase winding excitation to guarantee the desired rotation direction. An appropriate rotor position estimation method is still needed to properly lock the current duration relative to the rotor position for the smooth rotation thereafter. The rotor position estimation method proposed during running condition is different from the one at standstill and is shown in Fig. 3. Two-level estimation is contained in the proposed algorithm. The first level compares the current in all phase windings and selects the phase having the largest current as the optimal phase. The purpose of this level is to select a suitable phase, so that the rotor position can be estimated in the high resolution region R2. In the second or a more detailed level, the controller proceeds to find the accurate rotor position based on the flux linkage and current of the selected optimal phase. The flux linkage integration can be implemented either by software or hardware. In this paper, the flux linkage calculation follows the discrete equation

$$\lambda(k) = \lambda(k-1) + \{V(k-1) - \frac{1}{2}\, R(i(k-1) + i(k))\} T_s \tag{3}$$

where $\lambda(k-1)$ and $\lambda(k)$ are the flux linkages at sampling instants $(k-1)$ and (k), $i(k-1)$ and $i(k)$ are the phase currents at sampling instants $(k-1)$ and (k), $V(k-1)$ is the command voltage applied to the phase winding at sampling instant $(k-1)$, and T_s is the sampling time.

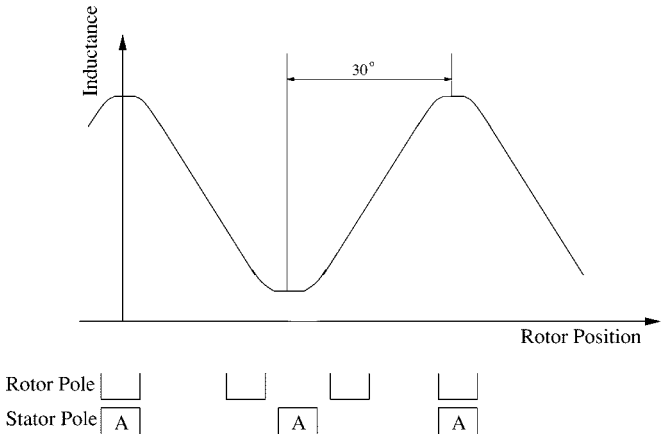

Fig. 4. Ideal inductance profile of an 8/6 SRM.

For accurate flux linkage calculation, it is better to synchronize (3) with the switching pulses (or the voltage excitation pulses). For example, if the switching frequency is 20 kHz, it is better to select 50 μs as the updating rate of (3). However, we can still accurately estimate the rotor position even if the flux linkage calculation is not synchronized with the switching pulses because of the robustness of the proposed algorithms. In our testing, the updating rate is fixed to 100 μs. The overall system has satisfactory performance when the switching frequency varies between 10–25 kHz.

To explain as to why during running condition the phase with the largest current is selected as the one for rotor position estimation, Fig. 4 shows the ideal unsaturated inductance profile of an 8/6 SRM in terms of rotor positions. Viewing Fig. 4, it can be noted that the current in the phase with no inductance variation while the rotor is rotating cannot generate any torque except for conduction losses. This implies that the phase current should be controlled high in the inductance increasing period and small or at zero in the constant inductance period so that high-efficiency operation of SRMs is achieved. The inductance increasing period usually starts several degrees after the totally unaligned position and ends several degrees before the totally aligned position. That is, the inductance increasing period corresponds to the high position resolution, region R2. Therefore, the phase having the largest current is selected as the optimal phase for rotor position estimation.

It should be further emphasized that successful operation of the proposed position estimation algorithm is heavily linked to the control algorithm for choosing appropriate turn-on and turn-off angles. The control algorithm guarantees the largest current occurs in the increasing inductance period. However, for most SRM control algorithms, we do expect the largest current in the inductance increasing period so that the system has a high efficiency.

D. Control Flow Chart

Combining the accurate initial rotor position with the above rotor position estimation algorithm, the SRM can then be reliably started. Because the initial rotor position is accurately found, no rotor position initialization (alignment) is needed and, thus, the starting hesitation is totally eliminated. Fig. 5 summarizes the control algorithms in a flow chart for starting and

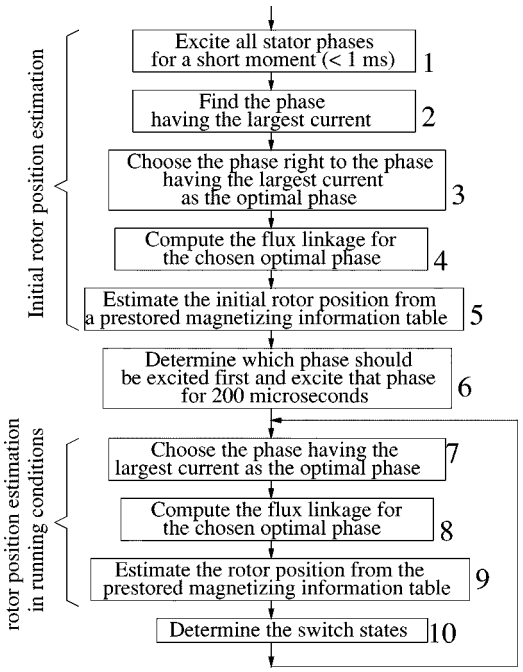

Fig. 5. Reliable sensorless starting of the SRM without starting hesitation.

continuous rotation without using rotor position sensor. In the figure, Blocks 1–5 are applied to estimate the initial rotor position as explained in Section III-B. Block 6 determines the phase which should be excite first to ensure the correct rotation. After the initial rotor position is estimated, the selected phase is excited for 200 μs to build up a current before the rotor position estimation algorithm is activated for running condition. This step guarantees an adequate current being established so as to avoid poor estimation accuracy. Blocks 7–9 are utilized to estimate the rotor position during running. Based on the estimated rotor position, block 10 determines the switch status for phase commutation.

IV. Computer Simulation and Experimental Results

Computer simulation and experimental investigation were conducted on an 8/6 SRM. The parameters and specifications of the SRM are given below as follows:

$$P = 0.5\,\text{hp}, \quad V_{\text{dc}} = 160\text{V}, \quad n = 3000\,\text{r/min},$$
$$R = 3.5\,\Omega, \quad L_u = 21.6\,\text{mH}, \quad L_a = 138.3\,\text{mH}$$

where L_a and L_u are the phase inductances at aligned and unaligned rotor positions, respectively. The measured magnetizing information of the machine is already shown in Fig. 2. In the following discussion, if not otherwise specified, the rotor position is in mechanical degrees relative to the aligned rotor position of phase A. Fig. 6 shows the system connection for the SRM control. From the measurement of dc-bus voltage and phase currents, the rotor position is estimated by the proposed estimation algorithm. The speed controller compares the command and estimated rotor speeds to generate the command current, turn-on, and turn-off angles [9]. Combining all angle and current information, the pulse modulator determines the gating signal to the inverter.

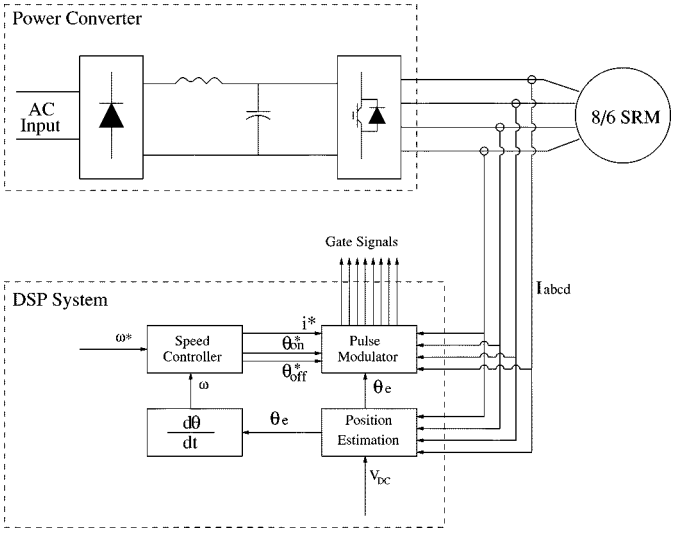

Fig. 6. System connection for the SRM control.

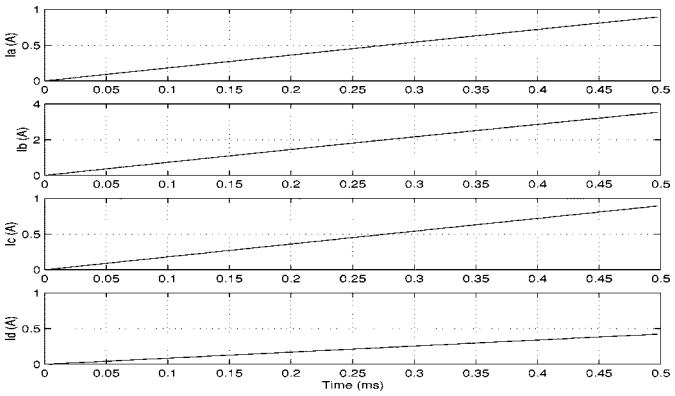

(a) Initial Rotor Position at 15 Degrees

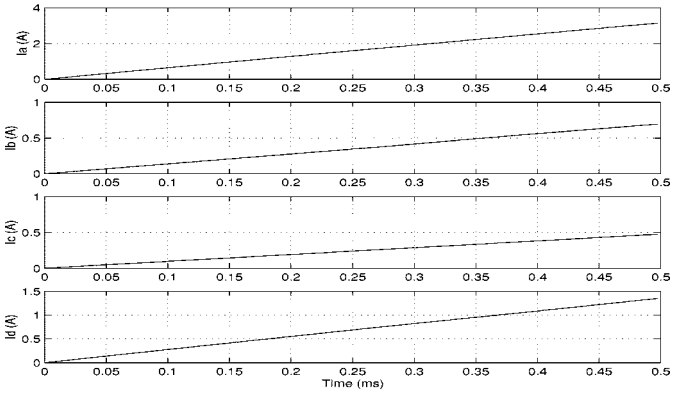

(b) Initial Rotor Position at 34Degrees

Fig. 7. Excitation current for initial rotor position estimation.

A. Computer Simulation Results

The algorithms for initial rotor position estimation at different initial rotor positions are first verified and the results are given in Fig. 7. The duration of excitation is 0.5 ms. In Fig. 7(a), the actual initial rotor position is arbitrarily given at 15°. Computer simulation shows that phase B has the largest current (3.5 A). According to the initial rotor position estimation algorithm, phase C is selected as the optimal phase. From the current and

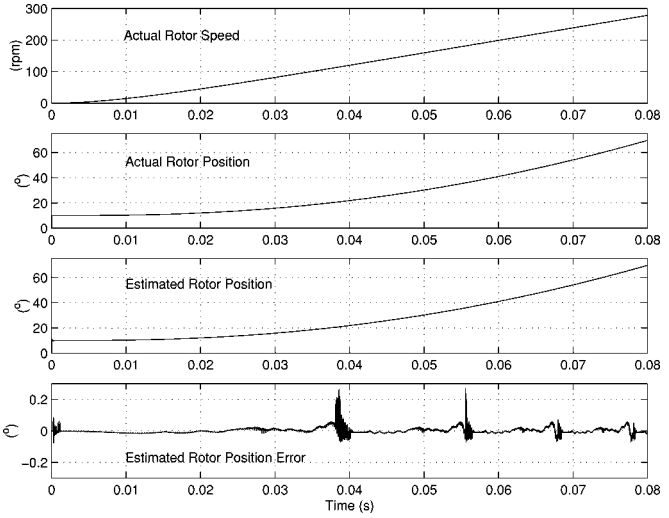

Fig. 8. Estimated rotor position during acceleration.

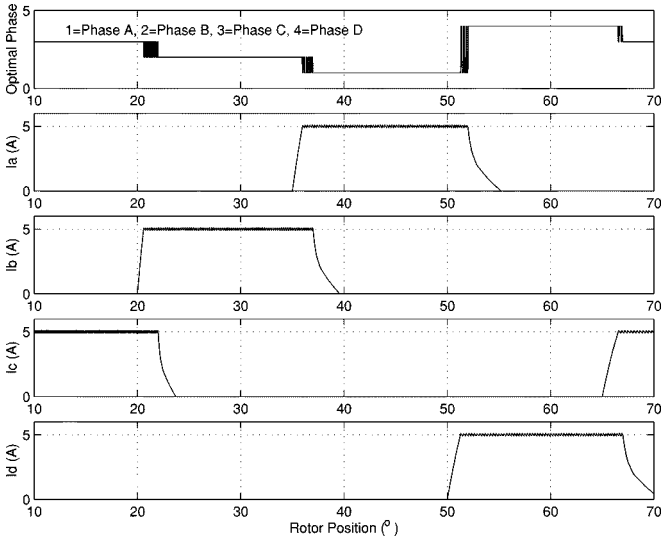

Fig. 9. Phase current during acceleration.

flux linkage of phase C, the initial rotor position of 15.4° is estimated. In Fig. 7(b), the actual initial rotor position is given at 34°. Computer simulation indicates that phase A has the largest current (3.1 A) and the optimal phase is B. The initial rotor position is again accurately estimated to be 34.1°. Fig. 7 also confirms two important assumption of the algorithm: 1) the excitation current will increase linearly if the duration of excitation (0.5 ms) is much less than the inverse of time constant of the stator winding circuit (25.3 s), so the flux linkage can be accurately calculated by the simplified (2) and 2) the optimal phase has a sufficient diagnostic signal. For example, the optimal phase has 0.85-A current in Fig. 7(a) and 0.70 A in Fig. 7(b).

With an arbitrary initial rotor position of 10° relative to the aligned rotor position of phase A, Figs. 8 and 9 show the computer simulation results during the starting of the SRM. In Fig. 8, the curves from top to bottom are the actual rotor

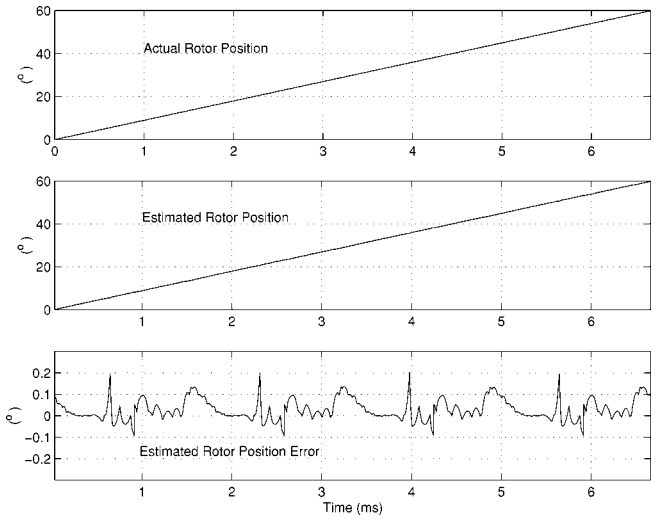

Fig. 10. Estimated rotor position at rotor speed of 1500 r/min.

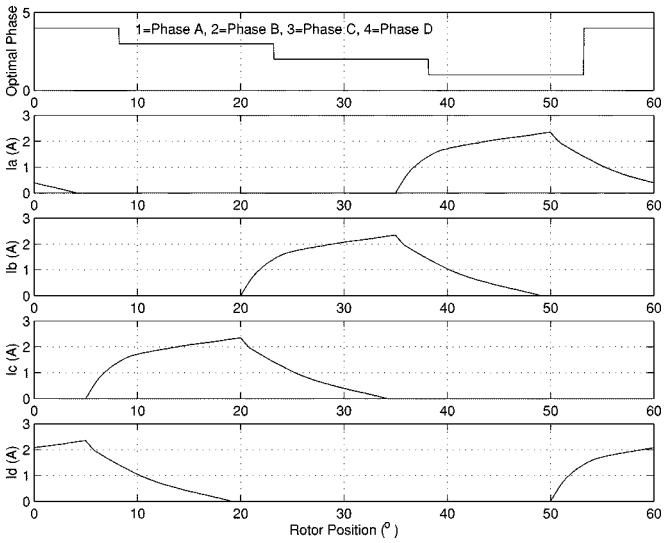

Fig. 11. Phase current at rotor speed of 1500 r/min.

speed, actual rotor position, estimated rotor position, and estimated rotor position error. When the SRM is accelerated from zero to 165 r/min, the estimated rotor position error is between -0.1 and $+0.25$ mechanical degrees. Fig. 9 shows the corresponding phase currents and the optimal phase for rotor position estimation during the starting process. During starting, the turn-on angle is fixed at 5° and the turn-off angle at 22° relative to the totally unaligned rotor position. It can be noted that the optimal phase is phase C for the rotor position between 10°–22°, phase B between 20.5°–37.2°, phase A between 35.5°–52.2°, and phase D between 51°–67.4°. Referring to Fig. 2, it can be observed that all rotor position estimation is conducted in the high-resolution region, R2, with the largest phase current. Therefore, the estimated rotor position has a high accuracy.

Fig. 9 indicates that there are overlapping intervals in which two phases are regulated to have the same current levels. For example, phases B and C are regulated to the same level from 20.5° and 22°. During this overlap interval, either phase B or C can be selected as the optimal phase for rotor position estimation. If allowed (with fast DSP), we can conduct the position estimation from both phases. The final estimated position is then obtained be averaging the two results from both phases, which will further increase the position estimation accuracy during overlapping intervals.

To verify that the above rotor position estimation method works reliably at high speed, the rotor speed is fixed at 1500 r/min in the computer simulation, and the results are shown in Figs. 10 and 11. The turn-on angle is the same as before, but the turn-off angle reduced to 20° to prevent negative torque production. The rotor position estimation is conducted for the rotor position between 8.0°–23° with respect to the unaligned rotor position of the selected optimal phase. The estimation error is between -0.1 and $+0.2$ mechanical degrees, as shown in Fig. 10. Comparing Fig. 8 with Fig. 10, it can be noted that the estimated rotor position has even higher accuracy at rotor speed of 1500 r/min than that during the starting stage because the rotor position estimation is conducted in a better region in the λ–i plane with the highest resolution. The result also verifies that determining the optimal phase is critical for the high accuracy of rotor position estimation.

B. Experimental Results

Fig. 12 presents the testing results from the simulated 8/6 SRM at different initial rotor positions. The actual initial rotor position is at 12° in Fig. 12(a), 25° in Fig. 12(b), and 40° in Fig. 12(c), respectively. In these figures, the top trace is the rotor speed, the middle the estimated rotor position, and the bottom the measured phase current. The initial excitation and rotor position estimation takes 0.54 ms with the Motorola DSP56005-based controller. In 0.35 s, the SRM is accelerated to 1200 r/min, regardless of where the initial rotor position is. The experimental results also confirm the computer simulation that the starting procedure described in Fig. 5 works well and can start the SRM at any initial rotor position without any starting hesitation. To verify that the method is not affected by load conditions, in the experiment, we repetitively stall the SRM by applying a large load torque to the rotor shaft through the dynamometer; nevertheless, the SRM recovers from stalling to the set speed as soon as the stall torque is removed. Fig. 13 shows the starting performance with a heavy load (70% of rated torque). In the figure, the initial rotor position is arbitrarily set to 20°. Again, the SRM can be reliably started without starting hesitation.

To verify the effectiveness of the estimation and control algorithms in a more comprehensive operating condition, Fig. 14 shows the four-quadrant operation of the SRM with the proposed algorithms. When the rotor speed decelerates from $+3000$ r/min (or -3000 r/min) to zero, the SRM works in the regenerative mode; and when the rotor speed accelerates from zero to $+3000$ r/min (or -3000 r/min), the SRM works in the motoring mode. Note that, in the SRM regenerative operation mode, the principles of the rotor estimation remain the same as those in the motoring mode. However, the current is commanded to the inductance decreasing period. It is evident

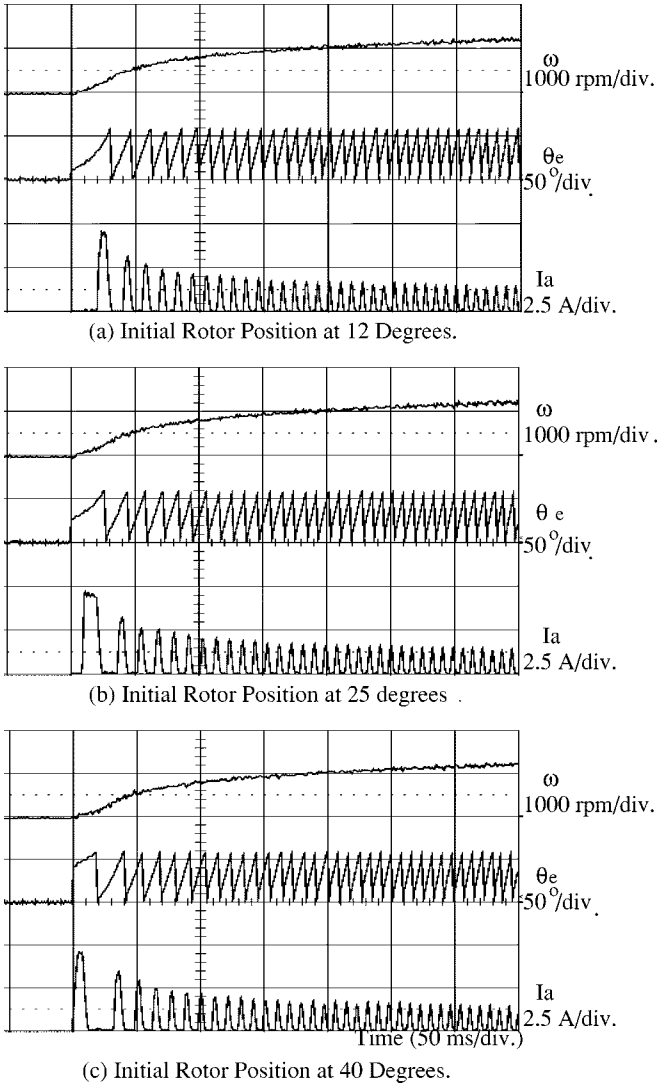

Fig. 12. SRM starting at different initial rotor positions.

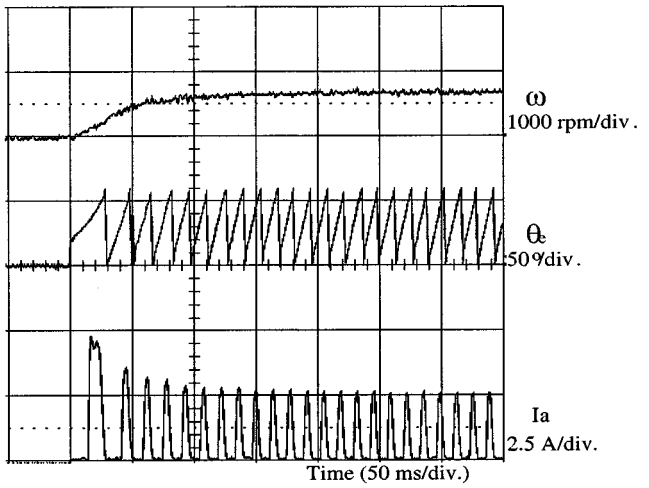

Fig. 13. SRM starting with 70% of rated torque.

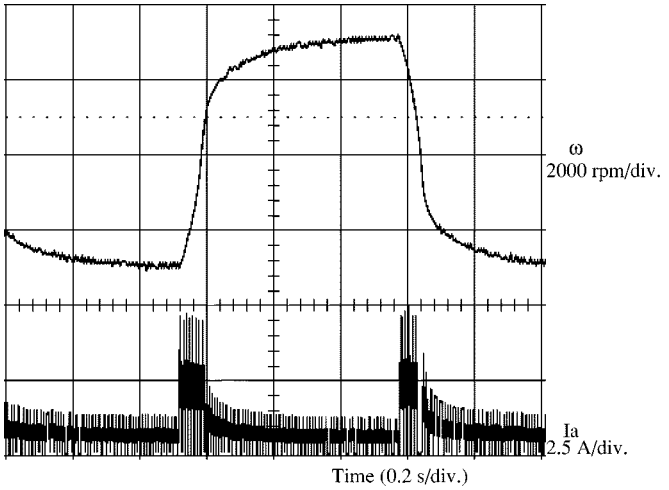

Fig. 14. Four-quadrant operation without position sensor.

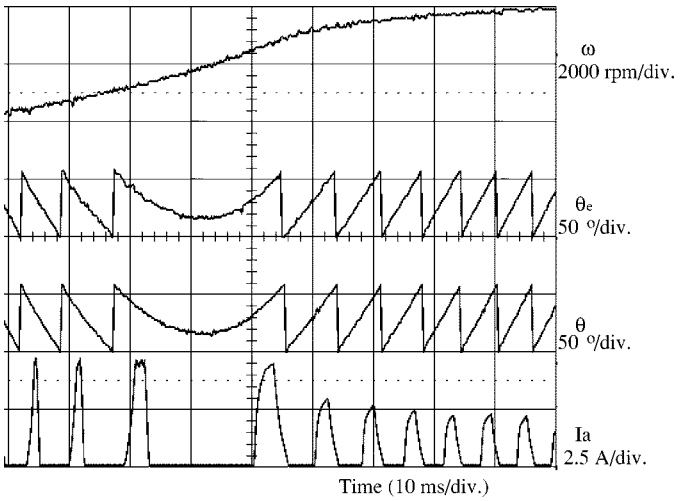

Fig. 15. Position estimation during rotating reversing.

that the proposed estimation and control algorithms are very effective over a wide range of operating conditions. Fig. 15 shows the details of the rotor position estimation performance during speed zero crossing. From the top to the bottom, the traces show the rotor speed, estimated rotor position, actual rotor position from optical encoder, and actual phase current. It should be pointed out that the actual rotor position is displayed here only for comparison with the estimated rotor position, and the control is completely based on the estimated rotor position. Comparing the estimated rotor position with the actual rotor position, it can be noted that the rotor position is accurately detected during speed transitions including zero speed. This result fully verifies that the SRM works reliably in four-quadrant operation without using a rotor position sensor.

V. Conclusions

Novel methods for rotor position estimation both at standstill and during running conditions have been presented in the paper. By applying a dc pulse voltage to the stator phase windings for a short moment (0.5 ms), the initial rotor position can be accurately estimated. Combining the accurate initial rotor position with the novel rotor position estimation algorithm during running, the SRM can be started at any initial rotor position without starting hesitation. Both computer simulation and experimental

results verified that the control algorithm guarantees the SRM a reliable and high performance over a wide range of operation conditions. Future work includes expanding the SRM capabilities of hesitation free and sensorless control to the speed range up to 100 000 r/min.

REFERENCES

[1] P. P. Acarnley, R. J. Hill, and C. W. Hooper, "Detection of rotor position in stepping and switched motors by monitoring of current waveforms," *IEEE Trans. Ind. Electron.*, vol. 32, pp. 215–222, June 1985.

[2] S. K. Panda and G. A. J. Amaratunga, "Waveform detection technique for indirect rotor-position sensing of switched-reluctance motor drives—Part 1: Analysis," *Proc. Inst. Elect. Eng.*, pt. B, vol. 140, no. 1, pp. 80–88, 1993.

[3] W. F. Ray and I. H. Al-Bahadly, "Sensorless methods for determining the rotor position of switched reluctance motors," in *Conf. Rec. IEE EPE Conf.*, Brighton, U.K., 1993, pp. 7–13.

[4] A. Cheok and N. Ertugra, "A model free fuzzy logic based rotor position sensorless switched reluctance motor drives," in *Conf. Rec. IEEE-IAS Annu. Meeting*, San Diego, CA, 1996, pp. 76–83.

[5] L. Xu and J. Bu, "Position transducerless control of switched reluctance machine with minimum magnetizing input," in *Conf. Rec. IEEE-IAS Annu. Meeting*, New Orleans, LA, 1997, pp. 533–539.

[6] G. Gallegos-Lopez, P. C. Kajr, and T. J. E. Miller, "A new sensorless method for switched reluctance motor drives," in *Conf. Rec. IEEE-IAS Annu. Meeting*, New Orleans, LA, 1997, pp. 564–570.

[7] M. Ehsani, I. Husain, and A. B. Kulkarni, "Elimination of discrete position sensor and current sensor in switched reluctance motor drives," *IEEE Trans. Ind. Applicat.*, vol. 28, pp. 128–134, Jan./Feb. 1992.

[8] M. Ehsani, I. Husain, S. Mahajan, and K. R. Ramani, "New modulation encoding techniques for indirect rotor position sensing in switched reluctance motors," *IEEE Trans. Ind. Applicat.*, vol. 30, pp. 85–91, Jan./Feb. 1994.

[9] J. Bu, "High performance position sensorless control of switched reluctance machines over a wide speed range," Ph.D. dissertation, Dep. Elect. Eng., The Ohio State University, Columbus, 1998.

[10] J. P. Lyons, S. R. MacMinn, and M. A. Preston, "Flux/current methods for SRM rotor position estimation," in *Conf. Rec. IEEE-IAS Annu. Meeting*, 1991, pp. 482–487.

[11] W. D. Harris and J. H. Lang, "A simple motion estimator for variable reluctance motors," in *Conf. Rec. IEEE-IAS Annu. Meeting*, 1988, pp. 281–286.

[12] S. R. MacMin, W. J. Rzesos, P. M. Szczensy, and T. M. Jahns, "Application of sensor integration techniques to switched reluctance motor drives," *IEEE Trans. Ind. Applicat.*, vol. 28, pp. 1339–1344, Nov./Dec. 1992.

Jianrong Bu (S'96–M'98) was born in China. He received the B.S.E.E. and M.S.E. degrees from Southeast University, China, and the Ph.D. degree from The Ohio State University, Columbus, in 1984, 1987, and 1998, respectively, all in electrical engineering.

He is currently a Project Leader with Emerson Drive Solutions, Minneapolis, MN. His research interests include DSP/microprocessor-based servo control systems, power electronics, high-performance servo drives, and firmware design.

Dr. Bu was a Motorola University Microprocessor Design Contest winner in 1998.

Longya Xu (S'89–M'90–SM'93) was born in Hunan, China. He graduated from Shangtan Institute of Electrical Engineering, China, and received the B.E. degree from Hunan University, China, and the M.S. and Ph.D. degrees from the University of Wisconsin, Madison, in 1970, 1982, 1986, and 1990, all in electrical engineering.

From 1982 to 1984, he was a Researcher for Linear Electric Machines in the Institute of Electrical Engineering, Sinica Academia of China. Since he came to the U.S., he has served as a Consultant to several companies, including Raytheon, U.S. Wind Power Company, Pacific Scientific, General Motors, Ford, and Unique Mobility Inc. In 1990, he joined the Department of Electrical Engineering, The Ohio State University, Columbus, where he is presently an Associate Professor. His research and teaching interests include dynamic modeling and optimally combined design of electrical machines with power converters for variable-speed generating and drive systems, and advanced control theory and DSP implementation applied to variable-speed systems.

Dr. Xu received the 1990 First Prize Paper Award from the Industrial Drives Committee of the IEEE Industry Applications Society (IAS). In 1991, he won a Research Initiation Award from the National Science Foundation. He was also a recipient of Lumley Research Awards in 1995 and 1998 for his research accomplishments from the College of Engineering, The Ohio State University. He is currently serving as the Chairman of the Electric Machines Committee of the IAS and as an Associate Editor of the IEEE TRANSACTIONS ON POWER ELECTRONICS.